Article

Time-Dependent Retention of a Mixture of Cs(I), Sm(III), Eu(III) and U(VI) as Waste Cocktail by Calcium Silicate Hydrate (C-S-H) Phases

Kristina Brix [ID], Aaron Haben and Ralf Kautenburger *[ID]

WASTe Group, Inorganic Chemistry, Saarland University, 66123 Saarbrücken, Germany; kristina.brix@uni-saarland.de (K.B.); aaron.haben@uni-saarland.de (A.H.)
* Correspondence: ralf.kautenburger@uni-saarland.de

Abstract: In the context of the safe storage of high-level radioactive waste, the time-dependent retention of a waste cocktail (WC) consisting of Zr(IV), Mo(VI), Ru(III), Pd(II), Cs(I), Sm(III), Eu(III) and U(VI) was studied on the commercially available C-S-H phase Circosil®. The herein presented results focus on Cs(I), Sm(III), Eu(III) and U(VI). Precipitation and wall adsorption studies in the absence of the solid phase show only a small amount of precipitation for Sm(III) and Eu(III) ($34 \pm 18\%$) in the high-saline diluted Gipshut solution (DGS, pH 10.6, I = 2.6 M). For Cs(I) and U(VI), no precipitation was observed. In 0.1 M NaCl (pH 10.9), the measured retention could completely be attributed to wall adsorption for all four elements. The obtained R_d values for the time-dependent retention of Sm(III), Eu(III) and U(VI) on Circosil® of 10^5 to 10^6 L·kg^{-1} are in good agreement with the literature. For Cs(I) in the strongly saline background electrolytes, slightly higher R_d values of up to $8 \cdot 10^2$ L·kg^{-1} were determined for the crystalline Circosil® compared to the wet chemical C-S-H phases. Overall, the commercial product Circosil® is suitable as an alternative to synthesised C-S-H phases to observe trends in the retention behaviour of these elements. Comparison between both background electrolytes shows an increase in the amount and velocity of retention for all four elements with decreasing salinity. This confirms adsorption processes as the fastest and initial retention mechanism. Precipitation or incorporation of Eu(III), Sm(III) and U(VI) cannot be ruled out in the long term. Comparing the kinetic of this WC study to single-element studies in the literature, a longer uptake time to reach a steady state of 7 d in 0.1 M NaCl and 28 d in DGS instead of <1 d was observed for Eu(III) and Sm(III). The situation for Cs(I) is similar. This indicates competing effects between the different WC elements for adsorption sites on the C-S-H phases.

Keywords: C-S-H phase; waste cocktail; high-level radioactive waste; caesium; europium; samarium; uranium; kinetic study; ICP-MS

1. Introduction

Cement-based materials are going to be used in repositories for high-level radioactive waste (HLW) worldwide. They will be used as construction or sealing material for their physical and chemical stability and their ability to immobilise hazardous substances [1–3]. Calcium silicate hydrate (C-S-H) phases are the major hydration product of hardened cement and are mainly responsible for the retention of anions or cations [3]. C-S-H phases are mostly amorphous and degrade over time in contact with aqueous media. Due to leaching of Ca(II), the calcium to silicon ratio (C/S) decreases within approximately 36,000 years from 1.5 to 0.8 [4]. The resulting pore water has an alkaline pH between 12.5 and 10 decreasing with decreasing C/S ratio. The alteration of the C-S-H phases is very complex due to a lot of dissolution and precipitation processes taking place and the amorphousness of the material overall [3,5].

C-S-H phases used for retention experiments in the context of an HLW repository are mainly synthesised wet chemical or hydrothermal. Precursors are usually CaO and

SiO_2 which are mixed via a "direct reaction" method [1,6,7] with aqueous media like ultrapure water. Despite this simple preparation procedure, the pH values that naturally occur during equilibration with background electrolytes vary in the literature just like the retention for certain elements due to the complex processes involved in the formation and degradation [1,8,9]. At least, C-S-H phases are also sensitive to CO_2 [10–12]. $CaCO_3$ can be formed on the surface which lowers the adsorption potential.

The aim of this study is to investigate the time-dependent retention behaviour of a waste cocktail (WC) of elements relevant for HLW disposal on a stable, commercial C-S-H phase with defined structure: Circosil®, which consists mainly (88%) of tobermorite with C/S = 0.83 and intercalated SiO_2 (10%) with traces (<0.5% each) of Al-, Mg-, Fe-, Ti-, K-, Na-, Zr-, Mn- and Cr-containing minerals [13]. At the end of the degradation process, C-S-H phases stabilise at a C/S ratio of ~0.8 and mostly have a structure similar to amorphous, disordered tobermorite [3,5,14–17]. Due to the complexity of the degradation process and possible heat release from the HLW, even crystallisation of the C-S-H phases cannot be ruled out [18,19]. All of this makes Circosil® a possible stable analogue to natural aged C-S-H phases. The WC consists of U(VI) representing the main component of the HLW inventory. The WC also contains Zr(IV), which is used as cladding for fuel rods in nuclear reactors [20,21], and Sm(III) which can be used as a neutron adsorber in control rods [22,23]. Additionally, the possible fission products Mo(VI), Ru(III), Pd(II), Cs(I) and Eu(III) are contained in the WC whereas Eu(III) and Sm(III) also act as homologues to Am(III) and Cm(III) [24–26].

In this study, the focus lies on experiments at pH values > 10. These pH values are naturally obtained during the equilibration of C-S-H phases with aqueous media. The used background electrolytes are highly saline (I = 0.1 M and 2.6 M) because host rocks for potential HLW disposals may be salt formations or in contact with salt dome deposits which results in highly saline pore waters [27–29]. Retention studies with such ionic strengths are scarce [14,30–35]. We used diluted Gipshut solution (DGS, I = 2.6 M) which is a reference pore water of claystone in northern Germany and 0.1 M NaCl as a simple and lower-saline comparative medium.

Finally, we present the retention results of Cs(I), Sm(III), Eu(III) and U(VI) as part of the WC on Circosil® over 217 d and elucidate the retention mechanisms in the nanomolar concentration range. Since the HLW must be stored safely for hundreds of thousands of years, knowledge of the immobilisation mechanisms is mandatory. So far, several attempts have already been made in the literature to clarify the retention and binding mechanism of these elements on cementitious materials ([3] and references within). The results vary depending on the initial concentrations and used analytical method. For most of these WC elements, it is difficult to elucidate the mechanism in detail because precipitation could occur even in the nanomolar concentration range. Additionally, many analytical methods are not sensitive enough to detect analyte concentrations in the picomolar range, which remain in the liquid phase for many elements that adsorb strongly to the solid phases, such as Sm(III) or Eu(III). The amorphous and changing structure with C/S ratio of the C-S-H phases make solids analysis even worse. The possible retention mechanisms observed so far for the four elements of interest are shortly summarised in the following.

For Cs(I), mainly ion exchange processes come into charge as the binding mechanism because it does not precipitate under natural conditions. Incorporation was also observed by Iwaida et al. [36] at a very high Cs(I) concentration. As already mentioned, observations in the literature for the uptake of radionuclides on C-S-H phases may vary a lot. A clear dependence of the Cs(I) adsorption on the initial concentration was observed by Missana et al. [37]. This is a strong indicator for different binding sites. Meanwhile, Atkinson and Nickerson [38] found the sorption isotherm to be linear. Therefore, one to three different adsorption sites (ion exchange, outer-sphere and inner-sphere complexes) are suggested in the literature for Cs(I) adsorption on cementitious materials [39–43].

For Eu(III), and Sm(III) as chemically very similar rare earth elements (and as homologues to Am(III) and Cm(III)), three retention mechanisms on cementitious materials

or C-S-H phases are proposed in the literature: adsorption, incorporation and precipitation [14,26,44–48]. Each of these studies observed high up to quantitative retention for both elements. This is either explained by the high affinity of the three valent cations to the negatively charged surface of the adsorbent material or precipitation due the alkaline background electrolyte.

Adsorption on the negatively charged surface of C-S-H phases seems unlikely for U(VI) at pH > 10 because it forms negatively charged carbonate or hydroxy complexes [30,49–51]. Nevertheless, high retention of U(VI) on cementitious materials is observed in many studies. It occurs through precipitation [2,9], incorporation [52], direct surface complexation [2,49,51,53,54] or ternary surface complexes involving Ca(II) [30,55,56]. Tits et al. [57] even observed three U(VI) species in their study which they attributed to surface complexation, an incorporated species and a uranate-like precipitate.

Altogether, the precipitation and wall adsorption experiments performed in this study, as well as different saline background electrolytes, WC elements as competing ions and the dynamic behaviour during the kinetic study, provide new insights into the retention mechanisms of Cs(I), Sm(III), Eu(III) and U(VI) on C-S-H phases.

2. Materials and Methods

2.1. Chemicals and Standards

All solutions were prepared with ultrapure water (0.055 µS·cm^{-2}) from a PURELAB® Chorus 1 ultrapure water filtration unit (Elga LabWater, High Wycombe, UK). For the preparation of the background electrolytes, NaCl, CaCl$_2$, Na$_2$SO$_4$ and KCl salts of premium-grade quality (EMSURE®) from the company Merck (Darmstadt, Germany) were used. Sc (1 g·L^{-1}, Alfa®, Karlsruhe, Germany) and Ho (1 g·L^{-1}, Merck Certipur®, Darmstadt, Germany) served as internal standards and HNO$_3$ (ROTIPURAN® Supra 69%, Carl Roth, Karlsruhe, Germany) for acidifying the measurement solutions for mass spectrometry with inductively coupled plasma (ICP-MS). To prepare the samples and the calibrations for the measurements, the following elemental standards were used: Si(IV) (10 g·L^{-1}, AccuStandard, New Haven, CT, USA), Ca(II) (1 g·L^{-1}, Merck Certipur®, Darmstadt, Germany), Zr(IV) (10 g·L^{-1}, Merck Supelco®, Darmstadt, Germany), Mo(VI) (1 g·L^{-1}, Fluka, Buchs, Switzerland), Ru(III) (1 g·L^{-1}, Merck, Darmstadt, Germany), Pd(II) (1 g·L^{-1}, Fluka, Buchs, Switzerland), Cs(I) (1 g·L^{-1}, AccuStandard, New Haven, CT, USA), Sm(III) (1 g·L^{-1}, Alfa Aesar Specpure®, Karlsruhe, Germany), Eu(III) (10 g·L^{-1}, Agilent, Kingstown, MD, USA) and U(VI) (1 g·L^{-1}, AccuStandard, New Haven, CT, USA). The C-S-H phases used are commercially available Circosil® 0.1 from Cirkel (Emsdetten, Germany). NaOH (Suprapur® 30%, Merck, Darmstadt, Germany) and HCl (HCl 30% Suprapur®, Merck Supelco®, Darmstadt, Germany) were used to adjust the desired pH of the precipitation and wall adsorption experiments.

2.2. Experiments and ICP-MS Samples

For the batch experiments, the two electrolytes 0.1 M NaCl and DGS (2.5 M NaCl, 0.02 M CaCl$_2$·2H$_2$O, 0.008 M Na$_2$SO$_4$ and 0.005 M KCl) were prepared.

For the kinetic experiments, 800 mg Circosil® were weighed in 250 mL LDPE bottles and 200 mL of the respective electrolyte was added (S/L = 4 g·L^{-1}). After 7 d equilibration in a horizontal shaker (Promax 1020 platform shaker, Heidolph Instruments, Schwabach, Germany), the pH was measured. It settled naturally to 10.9 in 0.1 M NaCl and 10.6 in DGS. According to Altmaier et al. [58], a pH correction of +0.5 was made in the high-saline DGS. Afterwards, the analytes (Zr(IV), Mo(VI), Ru(III), Pd(II), Cs(I), Sm(III), Eu(III) and U(VI)) were added at a concentration of 500 nmol·L^{-1}. Changes in the pH values due to the addition of acidic element standards were corrected with NaOH and adjusted to the former value of 10.9 or 10.6, respectively. Sampling of 1 mL each was performed after 1 h, 1 d, 3 d, 7 d, 14 d, 28 d, 56 d, 112 d, 168 d and 217 d. Each experiment was prepared in independent triplicates. Reference experiments without analyte were performed for background and leaching correction.

For the wall adsorption studies, polypropylene (PP) centrifuge tubes (Ultra-High Performance Centrifuge Tube, VWR International, Darmstadt, Germany) were filled with either 10 mL 0.1 M NaCl or DGS. After that, Zr(IV), Mo(VI), Ru(III), Pd(II), Cs(I), Sm(III), Eu(III) and U(VI) were added at the concentration of 500 nmol$\cdot$L^{-1}. To mimic the amounts of Si(IV) and Ca(II) leached by Circosil®, 1 mg$\cdot$L^{-1} each was added and additionally the pH was adjusted analogous to the kinetic study (0.1 M NaCl: 10.9; DGS: 10.6). After 7 days, 1 mL of sample was taken from each, and the lowest part of the PP tube, holding 1 mL, was removed and discarded. The upper part of the tube was soaked in 5% HNO$_3$ for at least one hour. Afterwards, this solution was also sampled.

2.3. The ICP-MS System

To quantify the samples with 0.1 M NaCl as background electrolyte, the WC elements were analysed by ICP-MS (Agilent 8900 ICP-QQQ, Santa Clara, CA, USA) using an Agilent SPS4 autosampler and a high matrix introduction system for higher salt concentrations up to 3% (HMI, Agilent) via a standard method.

The ionic strength of the DGS is higher than the commercial system can handle. Therefore, a transient ICP-MS method according to Hein et al. [59] was used. For this purpose, a 7500cx ICP-MS (Agilent, Santa Clara, CA, USA) was used with a CETAC autosampler (ASX 500) and an HMI system (Agilent). This method allows quantification of elements in up to 5 M saline solutions without further dilution or sample cleanup steps. Therefore, a supplemental solution is used to ensure a constant flow to the nebuliser (which also results in an on-line sample dilution of about 1:4), the sample acquisition time is shortened to 10 s and time-resolved measurements are performed.

All ICP-MS measurement solutions were prepared to a total volume of 10 mL and the solutions contained 5% HNO$_3$ and 10 μg$\cdot$L^{-1} each of Sc and Ho as internal standards. The quantification for both methods was performed by external calibration with concentrations from 0.001 to 20 μg$\cdot$L^{-1}.

3. Results

3.1. Precipitation and Wall Adsorption

Concerning the retention of heavy metals, many different processes can play a role. To differentiate between the influence of the adsorbent material and precipitation due to oversaturation or wall adsorption on the PP tubes in the alkaline pH range, batch experiments in the binary system (background electrolyte and analytes) and in the ternary system (C-S-H phase, background electrolyte and analytes) were conducted.

For all investigated elements, precipitation and wall adsorption were investigated as competing processes to the immobilisation on the C-S-H phase. Sm(III) and Eu(III) tend to precipitate at high pH values as hydroxides or carbonates [60–62] whereas the critical phases for U(VI) are Na$_2$U$_2$O$_7$ and CaUO$_4$ [3,63]. Cs(I) does not precipitate under natural conditions.

The results in the binary system (without adsorbent material) can be seen in Figure 1. Sm(III) and Eu(III) are almost quantitatively removed out of both background electrolytes ($\geq$95%). Additionally, wall adsorption or precipitation on the tube wall plays a major role in DGS with 93 $\pm$ 4% (Eu(III)) and 92 $\pm$ 4% (Sm(III)) in 0.1 M NaCl and 65 $\pm$ 19% (Eu(III)) and 64 $\pm$ 18% (Sm(III)). The smaller amount in DGS can be explained by wall saturation with ions from the background electrolyte.

For U(VI), only a low retention of 13 $\pm$ 2% in 0.1 M NaCl and 4 $\pm$ 4% in DGS can be observed. In DGS, the retention can be completely described by wall adsorption or wall precipitation. In 0.1 M NaCl, the share of wall adsorption is only 8 $\pm$ 1%. This agrees with the findings of Baqer et al. [54] that the nucleation kinetic of U(VI) is too slow to take place in most ordinary laboratory experiments.

The clear differences between Eu(III), Sm(III) and U(VI) in the precipitation/wall adsorption behaviour can be explained by the speciation in solution. U(VI) forms the two-fold-charged uranyl cation determining complexation and speciation behaviour whereas

for Eu(III) and Sm(III) the three-fold-charged cations are defining. At pH 10.5–11, U(VI) forms negatively charged species in solution (mainly $UO_2(OH)_3^-$ or $UO_2(CO_3)_3^{4-}$) which tend not to adsorb on the potential negatively charged tube wall [30]. The main species for Eu(III) are $Eu(OH)_3$ and $Eu(CO_3)_2^-$ [64] which have a higher affinity for wall adsorption under these conditions.
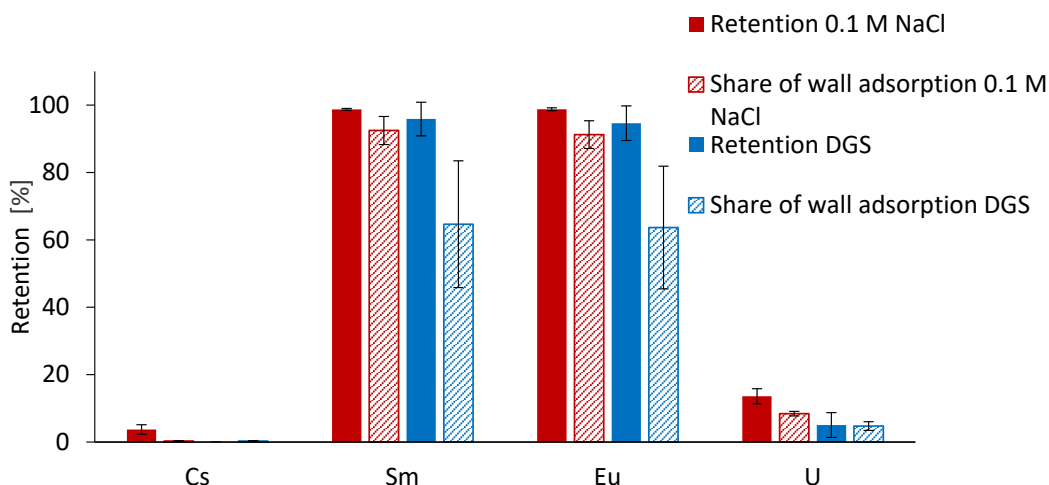
Figure 1. Retention of Cs(I), Sm(III), Eu(III) and U(VI) (initial concentration: $1 \cdot 10^{-7}$ mol·L^{-1}) after 7 d in 0.1 M NaCl (red, pH 10.9) and diluted Gipshut solution (DGS, blue, pH 10.6) and the share of wall adsorption (hatched) in the binary system (background electrolyte and analytes), also in the presence of $1 \cdot 10^{-7}$ mol·L^{-1} Zr(IV), Mo(VI), Ru(III) and Pd(II), respectively, and 1 mg·L^{-1} Si(IV) and Ca(II).

As expected, no relevant precipitation or wall adsorption can be detected for the single-charged Cs(I). Even in the lower saline 0.1 M NaCl solution, the excess of Na(I) is 200,000-fold more than that of Cs(I). It can be assumed that this excess saturates the tube wall.

In the presence of Circosil® (Figure 2), the retention of Cs(I) and U(VI) increases strongly: in 0.1 M NaCl from $3 \pm 1\%$ to $59 \pm 1\%$ for Cs(I) and from $13 \pm 2\%$ to $97 \pm 1\%$ for U(VI), respectively. In DGS, the immobilisation increased for Cs(I) from 0% to $14 \pm 3\%$ and for U(VI) from 4 ± 4% to $98.7 \pm 0.3\%$.
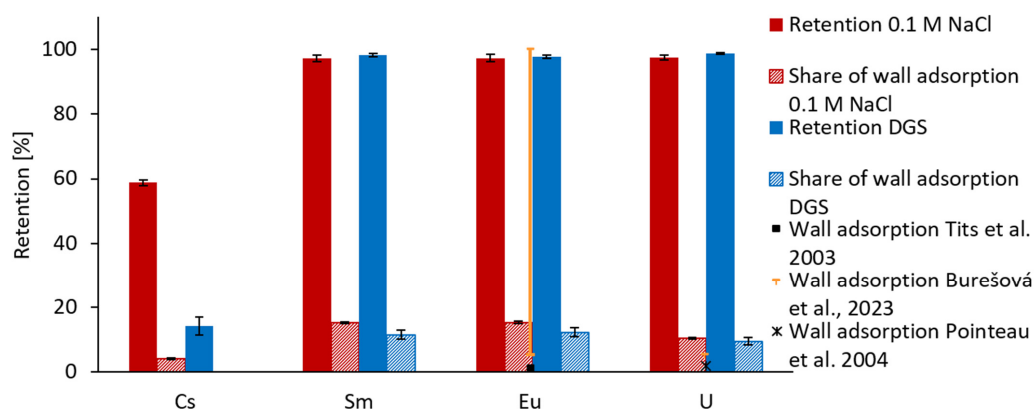
Figure 2. Retention of initial $1 \cdot 10^{-7}$ mol·L^{-1} Cs(I), Sm(III), Eu(III) and U(VI) on Circosil® (7 d equilibrium time) in 0.1 M NaCl (red, pH 10.9) and diluted Gipshut solution (DGS, blue, pH 10.6) and the share of wall adsorption (hatched), also in the presence of Zr(IV), Mo(VI), Ru(III) and Pd(II). Data points refer to wall adsorption from previous studies: <1% and 6.5%–100% for Eu(III) [26,44] and <2% and <5% for U(VI) [44,51].

The amount of wall adsorption involved in the retention decreases to ≤15% for each element studied. Especially for Eu(III) and Sm(III), it can be clearly seen that the immo-bilisation on Circosil® is the preferred retention mechanism compared to wall adsorption

and classic precipitation in the binary system without adsorbent material. In the literature, wall adsorption of Eu(III) [26,44] and U(VI) [44,51] on PP tubes in the presence of C-S-H phases and hydrated cement paste was also investigated. While Tits et al. [26] observed wall adsorption <1% for Eu(III), the results gained by Burešová et al. [44] and Pointeau et al. [51] are similar to this study. They found only a small amount of U(VI) adsorbed on the wall (<2 or <5%, c(U(VI)) = $4 \cdot 10^{-9} - 7 \cdot 10^{-8}$ mol·L^{-1}). For Eu(III), the adsorbed amount was 6.5%–100% depending on the solid-to-liquid ratio and the present adsorbent material. Burešová et al. [44] explained it by the adsorption of cement or C-S-H colloids on the wall where Eu(III) or U(VI) is immobilised. The same observation was made in this study as even after centrifugation, small particles were visible in the upper part of the liquid phase and on the tube wall. These particles could either be C-S-H phase or leached SiO$_2$. So, the observed wall adsorption can be retention on the C-S-H phase which adhered on the wall until desorption with HNO$_3$.

These experiments show a clear involvement of Circosil$^{®}$ in the retention of all four elements. U(VI) and Cs(I) show almost no retention in the absence of the C-S-H phase, so surface precipitation may be excluded, and the retention should be driven by adsorption processes. Nevertheless, it is not possible to distinguish between adsorption or surface precipitation processes for Eu(III) and Sm(III). The wall adsorption observed for both elements in the absence of Circosil$^{®}$ could be attributed to wall precipitation of nanoscale solids due to the larger surface area on the wall of the PP tubes (approximately 36 cm^2) compared to the tube's bottom (approximately 2 cm^2). The surface of Circosil$^{®}$ is 65 m^2·g^{-1} [15] which equals 2.6 m^2 for the 40 mg used in the experiment. This exceeds the tube's surface by far and means the C-S-H phase is the preferred place for possible precipitation and adsorption.

3.2. Time-Dependent Retention of Cs(I)

A steady state is settled very fast by the time-dependent adsorption of $5 \cdot 10^{-7}$ mol·L^{-1} Cs(I) on Circosil$^{®}$ (Figure 3). After 7 d in 0.1 M NaCl and 3 d in DGS, an adsorption of $75 \pm 1\%$ or $14 \pm 1\%$ is reached, respectively. It does not change until 217 d in 0.1 M NaCl which shows an irreversible binding of Cs(I) on the C-S-H phase in this stationary experiment. In DGS, a slight decrease from 15% after 112 d to 9% after 217 d is visible. The three independent experimental rows show only slight variations of <3%. The influence of the background electrolyte's salinity on the Cs(I) adsorption can clearly be seen as the adsorption decreases strongly with the increased Na(I) concentration from 0.1 M NaCl to 2.5 M NaCl in DGS. This agrees with the literature [3,31,65]. Nevertheless, it is remarkable that adsorption of Cs(I) still takes place despite a 5-million-fold excess of Na(I) in DGS.
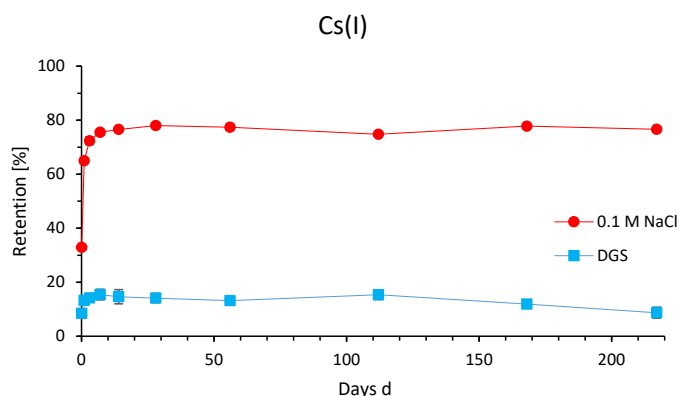
Figure 3. Time-dependent adsorption of initial $5 \cdot 10^{-7}$ mol·L^{-1} Cs(I) on Circosil$^{®}$ in 0.1 M NaCl (red dots, pH 10.9) and diluted Gipshut solution (DGS, blue squares, pH 10.6), also in the presence of Sm(III), Eu(III), U(VI), Zr(IV), Mo(VI), Ru(III) and Pd(II). Lines between the measurement points are only drawn for clarification.

These observations are in contrast with a recent kinetic study on a synthesised C-S-H phase (C/S = 1.08). There, in 0.1 M NaCl, Cs(I) adsorption was only remarkably detectable after 28 d (7 $\pm$ 0%) for the initial $5 \cdot 10^{-7}$ mol·L^{-1} Cs(I) and increased until the end of the experiment (112 d, 15 $\pm$ 2%) [14]. Not only was the kinetic much slower, the total amount of immobilised Cs(I) is also around five times lower than on the commercial C-S-H phase. In DGS, Cs(I) adsorbed on the synthesised C-S-H phase after 1 h and 1 d, but afterwards, no adsorption could be detected anymore [14]. This is also in contrast with the current study. A reason for this may be the differences in the C/S ratio. The capability of Cs(I) immobilisation increases with decreasing C/S ratio due to the decreasing amount of Ca(II) blocking potential binding sites [37,65–68]. With respect to the high Na(I) concentration, the $2 \cdot 10^{-2}$ mol·L^{-1} Ca(II) in DGS and the other competing WC elements, the lower C/S ratio of Circosil$^{\circledR}$ (0.83) cannot be the only explanation for this phenomenon. It also does not fit modelled data where an increase in the C/S ratio from 0.83 to 1.25 led to a decrease in Cs(I) adsorption from 37% to 23% in the micromolar concentration range [65]. The other difference between the C-S-H phases is the crystallinity and, consequently, the kind and amount of possible binding sites for Cs(I). Wet chemical synthesised C-S-H phases are amorphous and poorly crystalline [69] whereas the structure of the hydrothermal manufactured commercial product equals an 11-Å tobermorite [13]. This could enhance the Cs(I) adsorption capacities [69,70].

Three adsorption sites are considered in theoretical models for the Cs(I) uptake on C-S-H phases: ion exchange and surface complexation on weak or strong binding sites [37,39,43]. The latter have only a low capacity compared to the other sites. According to Duque-Redondo et al. [39], the weak sites represent outer-sphere and the strong sites inner-sphere surface complexes. In this study, it is very likely that the adsorbed Cs(I) is immobilised mainly on the strong binding sites via inner-sphere complexes. Because of the high hydration energy, these sites are considered non-accessible for most competing ions such as Na(I) or the elements present in the WC. Only K(I) from the DGS has access to these sites which contributes to the lowered adsorption in DGS compared to 0.1 M NaCl [41,71–73]. Also in molecular dynamics simulations, Cs(I) tends to adsorb as inner-sphere complexes on tobermorite [74]. Another hint for the Cs(I) adsorption on the strong sites is the immobilisation's irreversibility. Iwaida et al. [30] observed an incorporation in the C-S-H structure at high Cs(I) concentrations (1 mol·L^{-1}) which is also irreversible. Incorporation processes take place on a long timescale. So, it is not very likely to be the initial retention mechanism in this study where a steady state is reached after three to seven days. Nevertheless, a small decrease in Cs(I) adsorption in DGS is visible over time. It is possible that K(I) displace Cs(I) from the strong binding sites on a long timescale.

In the kinetic study of Missana et al. [37], a steady state of the Cs(I) adsorption on a C-S-H gel (C/S = 0.8) was already reached at the first measurement point after 1 d in deionised water. Also, Arayro et al. [66] calculated fast steady state settling of 1 d for Cs(I) on a modified 11-Å tobermorite. This contrasts with our results where the Cs(I) adsorption stays constant after 7 d (0.1 M NaCl) or 3 d (DGS). The difference can be explained either by the competing ions of the background electrolytes or by the elements of the WC competing for fast accessible binding sites such as ion exchange sites. This agrees with the results of Li and Pang [75]. They observed a characteristic adsorption time for Cs(I) on mortar in a high-saline pore solution (I = 0.23 M) of 0.44–0.6 d, but a quasi-steady state was only reached after 7 d. Furthermore, they also investigated the influence of Sr(II) on the time-dependent Cs(I) adsorption and found a small decrease in the adsorbed Cs(I) amount. As their background electrolyte already contained 40 mg·L^{-1} of Ca(II), the additional impact of $2.8 \cdot 10^{-10}$ mol·L^{-1} Sr(II) is remarkable. This highlights the importance of retention studies in the presence of possible competing ions not only from the background electrolyte but also from the radioactive inventory. Nevertheless, the investigated concentration of $5 \cdot 10^{-7}$ mol·L^{-1} of the WC elements may be too low to see a competing effect with Cs(I) compared to the concentrations of the background electrolyte's components because for

the Cs(I) adsorption on bentonite in similar media, an effect was only visible at an analyte concentration of $2.5 \cdot 10^{-4}$ mol·L^{-1} [31].

At least, the steady state of the Cs(I) adsorption on Circosil® is reached earlier in the higher-saline solution (DGS, 3 d) than in 0.1 M NaCl (7 d). This behaviour could be explained by the amount of adsorbed Cs(I). In 0.1 M NaCl, around 5 times more Cs(I) ($75 \pm 1\%$, $3.7 \cdot 10^{-7}$ mol·L^{-1}) is bound to Circosil® than in DGS ($14 \pm 1\%$, $7 \cdot 10^{-8}$ mol·L^{-1}). The strong binding sites with low capacity are not easily accessible, so the larger amount of Cs(I) which is able to get there in 0.1 M NaCl needs more time.

In Table 1, the distribution coefficients R_d [L·kg^{-1}] for Cs(I) are shown at different times in 0.1 M NaCl and DGS. The coefficient is normally written as K_d, representing the ratio of the element's amount bound to the solid and the amount in the liquid phase. Since precipitation of Sm(III), Eu(III) and U(VI) may not be completely excluded, all values are represented by R_d for consistency. The R_d values for Cs(I) in the literature are broadly scattered and depend mainly on the salinity of the background electrolytes, on the C/S ratio and the initial Cs(I) concentration but also on the absorbent material's structure [3]. In this study, they range between 100 and 900 L·kg^{-1} in 0.1 M NaCl with an average of 830 ± 60 L·kg^{-1} in the steady state after 7 d. The gained values are at the upper end of or even higher than the range reported in the literature despite the comparatively higher ionic strength [37,65]. As expected, the R_d values in DGS are with 23–46 L·kg^{-1} lower due to the high salinity and presence of a K(I) excess. The average value is 39 ± 7 L·kg^{-1}. Values in the same range were also found by Missana et al. [37] for C/S = 1.0 after equilibration in deionised water. Baur et al. [14] also observed lower R_d values in identical background electrolytes but with a higher C/S ratio (1.08). This leads to the conclusion that the C/S ratio and the structure of the C-S-H phase are more critical parameters for the Cs(I) adsorption than salinity or the initial concentration.
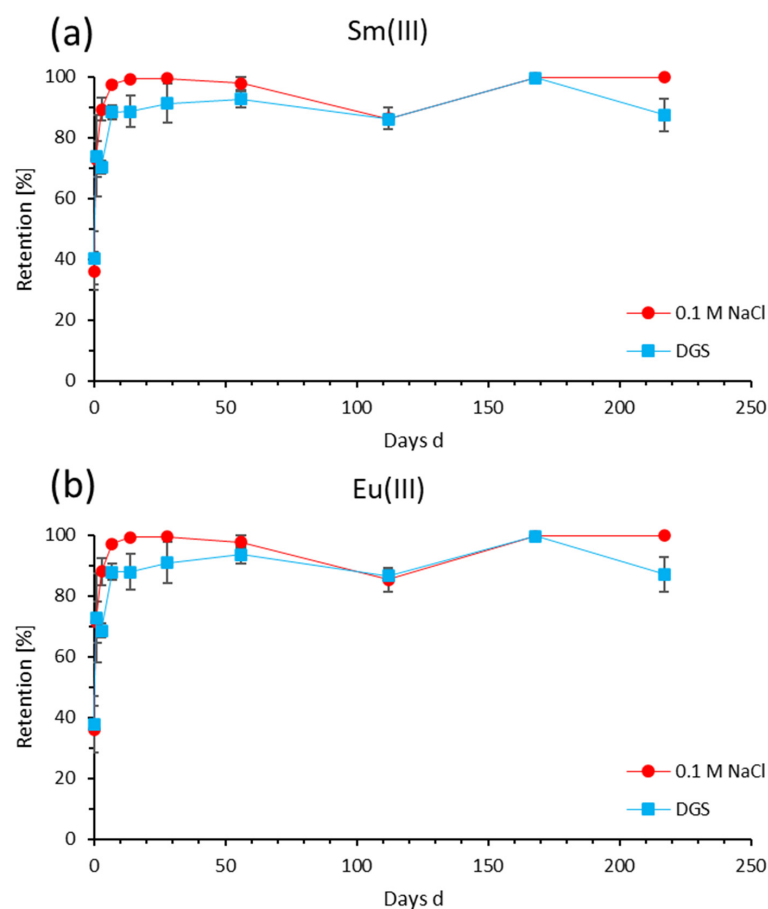
3.3. Time-Dependent Retention of Sm(III) and Eu(III)

The time-dependent retention of Eu(III) and Sm(III) on the commercial C-S-H phase Circosil® is shown in Figure 4. As both elements are trivalent actinides and the physical and chemical properties rarely differ, the retention behaviour is extremely similar. After 7 d of equilibration time, $97 \pm 1\%$ of the analytes are removed from the liquid phase in 0.1 M NaCl. The retention stays constant over the observed period with only one exception after 112 d where it decreases to $86 \pm 4\%$. The kinetic is slower and the overall retention of Sm(III) and Eu(III) is lower in DGS. Additionally, 7 d were needed to reach an immobilisation of $88 \pm 2\%$ which slowly increases further to $99.7 \pm 0.6\%$ after 168 d. Afterwards, the retention decreases to $87 \pm 6\%$ again.

Table 1. Distribution coefficients R_d for the retention of $5 \cdot 10^{-7}$ mol·L^{-1} Cs(I) on Circosil® in 0.1 M NaCl (pH 10.9) and diluted Gipshut solution (DGS, pH 10.6) at ten different sampling times (also in the presence of $5 \cdot 10^{-7}$ mol·L^{-1} Sm(III), Eu(III), U(VI), Zr(IV), Ru(III), Mo(VI) and Pd(II)).

Equilibration Time [d]	R_d(Cs(I)) in 0.1 M NaCl [10^3 L·kg^{-1}]	R_d(Cs(I)) in DGS [10^3 L·kg^{-1}]
0.04	0.123 ± 0.004	0.023 ± 0.004
1	0.46 ± 0.02	0.038 ± 0.002
3	0.65 ± 0.05	0.041 ± 0.004
7	0.77 ± 0.04	0.046 ± 0.007
14	0.82 ± 0.02	0.043 ± 0.009
28	0.89 ± 0.03	0.041 ± 0.006
56	0.86 ± 0.05	0.038 ± 0.006
112	0.74 ± 0.03	0.046 ± 0.006
168	0.88 ± 0.03	0.034 ± 0.004
217	0.82 ± 0.04	0.024 ± 0.006

Figure 4. Time-dependent retention of $5 \cdot 10^{-7}$ mol·L^{-1} Sm(III) (**a**) and Eu(III) (**b**) on Circosil® in 0.1 M NaCl (red dots, pH 10.9) and diluted Gipshut solution (DGS, blue squares, pH 10.6), also in the presence of Cs(I), U(VI), Zr(IV), Mo(VI), Ru(III) and Pd(II). Lines between the measurement points are only drawn for clarification.

A small drop in the immobilised amount of Sm(III) and Eu(III) can also be seen after 112 d (86 ± 2%) for both background solutions. The reproducibility of the measured data is worse in DGS with a standard deviation of >5% at five measurements points (15% after 1 d at maximum) than in 0.1 M NaCl (two measurement points >5%, 8% after 1 h at maximum). Despite the similar behaviour, the immobilisation of Sm(III) on Circosil® is slightly preferred over Eu(III). With only one exception (after 112 d in DGS), the retention of Sm(III) is up to 2 percentage points (pp) higher and the standard deviations lower at every measurement point than for Eu(III).

In the literature, three retention mechanisms are proposed for Eu(III): precipitation, incorporation and surface complexation [26,45,47,48]. The negative influence of increasing ionic strength on the retention behaviour in this study indicates retention mechanisms where competing effects play a role. This let incorporation or surface complexation appear to be the preferred mechanisms which was also observed by Mandaliev et al. [46]. Tits et al. [26] proposed precipitation followed by incorporation to be responsible for the retention of Cm(III) at pH 13.3. In this case, we would expect a positive influence of the salinity in our experiment. Nevertheless, the dynamic behaviour of Eu(III) and Sm(III) in this study after 56 d can be a hint for several retention processes taking place. Parts of the adsorbed lanthanides can slowly become incorporated in the C-S-H phase's structure. Precipitation, e.g., as Ln(OH)$_3$ or Ln$_2$(CO$_3$)$_3$ (Ln = lanthanide), cannot completely be ruled out on the longer timescale. The >70% immobilisation after 1 d for both elements hints to a fast process influenced by competing ions. Surface complexation fits this very well. The

slightly lower affinity for Eu(III) may be caused by competing effects between Eu(III) and Sm(III) or due to different ionic properties.

A comparison between this study and a kinetic study on a synthesised C-S-H phase (C/S = 1.08) shows similarities in the retention behaviour of Eu(III) [14]. It is immobilised fast and almost quantitatively. The retention stays dynamic over the observed timescale of 112 d. Despite this, the retention process for $5 \cdot 10^{-7}$ mol·L^{-1} Eu(III) is faster in DGS than in 0.1 M NaCl which is in contrast to the study presented here. The authors explained the Eu(III) retention mainly by precipitation, but no wall adsorption was investigated in their precipitation experiments. Their study was carried out at higher pH values (pH 12.5–13) than the present study. Eu(III) undergoes a change in speciation between pH 10.5 and 13 [64]. This can enhance the precipitation of Eu(III), e.g., as Eu(OH)$_3$. A retention >90% is reached after 1 d in 0.1 M NaCl and DGS [14] which contrasts with the current study where equilibration times of 7 d and 28 d were needed, respectively. In other studies, Eu(III) or Sm(III) retention of >90% on cementitious materials is reached within several minutes to 1 d [26,44,47,48,76]. Reasons for this may be the competition for binding sites between Eu(III), Sm(III) and other elements present in this study or higher analyte concentrations or pH values in the literature which favour precipitation.

In the kinetic study of Tits et al. [26] on C-S-H phases (C/S = 1) in a mixture of NaOH and KOH (I ~ 0.3 M), without trivalent competing ions, Eu(III) retention was also constant after 1 d of equilibration time. The R_d values were $60 \pm 30 \cdot 10^3$ L·kg^{-1} in the same order of magnitude as in the present study in 0.1 M NaCl after 14 d (Table 2). The R_d values in high-saline DGS are one order of magnitude lower. The high uncertainties, especially at high R_d values, result from the very low concentrations (c_{eq}) measured in the supernatant. After 217 d, the three measured concentrations in the 0.1 M NaCl supernatant for Sm(III) were $0.17 \cdot 10^{-9}$, $1.7 \cdot 10^{-9}$ and $1.9 \cdot 10^{-9}$ mol·L^{-1}. In absolute numbers, the resulting R_d values are $730 \cdot 10^3$, $72 \cdot 10^3$ and $67 \cdot 10^3$ L·kg^{-1}. This results in a deviation for R_d larger than the average value.

Table 2. Distribution coefficients R_d for the retention of $5 \cdot 10^{-7}$ mol·L^{-1} Sm(III) and Eu(III) on Circosil® in 0.1 M NaCl (pH 10.9) and diluted Gipshut solution (DGS, pH 10.6) at ten different sampling times (also in the presence of $5 \cdot 10^{-7}$ mol·L^{-1} Cs(I), U(VI), Zr(IV), Ru(III), Mo(VI) and Pd(II)).

| Equilibration Time [d]	R_d(Sm(III)) in 0.1 M NaCl [10^3 L·kg^{-1}]	R_d(Eu(III)) in 0.1 M NaCl [10^3 L·kg^{-1}]	R_d(Sm(III)) in DGS [10^3 L·kg^{-1}]	R_d(Eu(III)) in DGS [10^3 L·kg^{-1}]
0.04	0.14 ± 0.04	0.14 ± 0.05	0.18 ± 0.07	0.16 ± 0.06
1	0.7 ± 0.2	0.6 ± 0.2	0.9 ± 0.6	0.9 ± 0.6
3	2 ± 0.7	1.8 ± 0.7	0.60 ± 0.06	0.55 ± 0.06
7	9 ± 4	8.5 ± 3.4	1.9 ± 0.4	1.8 ± 0.4
14	37 ± 9	35 ± 8	2.3 ± 1.2	2.2 ± 1.1
28	41 ± 16	38 ± 13	4 ± 3	4 ± 3
56	11 ± 12	11 ± 11	3.4 ± 1.3	4 ± 2
112	1.6 ± 0.4	1.4 ± 0.4	1.6 ± 0.2	1.6 ± 0.3
168	79 ± 60	82 ± 66	>100 *	>50 *
217	290 ± 380	770 ± 1200	2 ± 1	2 ± 1

* At least one of the triplicates was below the detection limit.

Similar to the study of Baur et al. [14], the study by Tits et al. [26] was carried out at a significantly higher pH value (13.3) and the authors suggest precipitation as the first occurring retention mechanism. Häußler et al. [77] investigated the retention of $1 \cdot 10^{-8}$ mol·L^{-1} Am(III) on C-S-H phases with different C/S ratios and consequently different pH values in the range of 10.2–12.6. After 72 h of equilibration time, no relevant differences in the adsorption behaviour were noticeable with >98% retention for all experiments. The R_d values are $3 \cdot 10^4$ to $1 \cdot 10^6$ L·kg^{-1}, in agreement with the literature and in the range of this study. Häußler et al. [77] explained the retention with surface complexation on silanol groups as the chosen actinide concentrations are under the solubility limit. The

kinetic in the study of Häußler et al. [77] is faster than in the current study, independent of the pH value and with most likely surface complexation as the preferred retention mechanism. Similar observations were made by Pointeau et al. [47] where the amount of unadsorbed Eu(III) was under the limit of detection for every C/S ratio they investigated. This indicates a strong influence of the competing ions (WC and background electrolyte) on the retention kinetic of Eu(III) and Sm(III), which were not present in study of Häußler et al. [77] or Pointeau et al. [47].

3.4. Time-Dependent Retention of U(VI)

In Figure 5, the time-dependent retention of $5 \cdot 10^{-7}$ mol·L^{-1} U(VI) on Circosil® in 0.1 M NaCl and DGS can be seen. U(VI) has a faster retention kinetic than the other investigated WC elements.
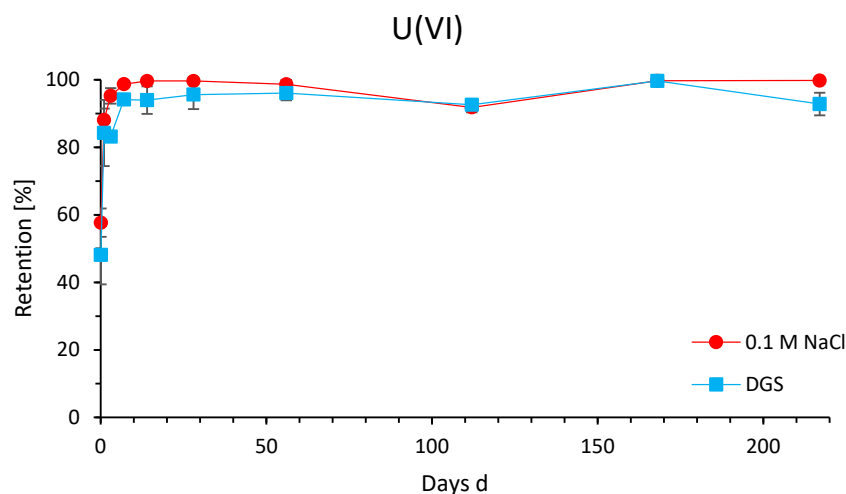
Figure 5. Time-dependent retention of $5 \cdot 10^{-7}$ mol·L^{-1} U(VI) on Circosil® in 0.1 M NaCl (red dots, pH 10.9) and diluted Gipshut solution (DGS, blue squares, pH 10.6), also in the presence of Cs(I), Sm(III), Eu(III), Zr(IV), Mo(VI), Ru(III) and Pd(II). Lines between the measurement points are only drawn for clarification.

In 0.1 M NaCl, the retention increased to >95% after 3 d and after 7 d a steady state of around 99% retention is reached. The retention in DGS is noticeably lower (mainly for the first 56 days) but a steady state with 94%–96% retention was also reached after 7 d. R_d values are >$1 \cdot 10^3$ L·kg^{-1} after 1 d of equilibration time (Table 3) in good agreement with the literature [9,14,44,49,51]. The influence of ionic strength on the retention of U(VI) in DGS is 3–5 pp lower than for Eu(III) and Sm(III), and especially compared to the adsorption of Cs(I). The solubility of U(VI) is controlled by CaUO$_4$ and Na$_2$U$_2$O$_7$ at pH > 9 [3,9,63]. The solubility limits are supposed to be 10^{-7} to 10^{-14} mol·L^{-1}. In the present study, the precipitation of U(VI) after 7 d of equilibration was investigated (Figure 1). Only <13% of the initial U(VI) were immobilised which excludes precipitation as a retention mechanism on the short timescale. This agrees very well with the study of Tits et al. [9] who found a steady state for the retention of U(VI) on C-S-H phases (C/S = 1.1) after 10 d of equilibration time. They also observed a small decrease in R_d values for U(VI) with increasing salinity of the background electrolyte and no precipitation of CaUO$_4$ in the nanomolar concentration range. Tits et al. [9] also observed that U(VI) uptake increases with increasing C/S ratio or Ca(II) concentration. They explained this by the formation of a Ca-U-bearing solid but were not able to determine a solubility limit in their sorption isotherm experiments. Recent studies have shown that the initial retention mechanism for U(VI) in this study and probably also in the older study of Tits et al. [8] is surface complexation of UO$_2$(OH)$_3$$^-$ or UO$_2$(OH)$_4$$^{2-}$ most likely via Ca(II) bridges [30,55,56,78]. Ca(II) adsorbs on deprotonated silanol groups on the C-S-H phase's edge where a hydroxy ligand of U(VI) can be attached. Since the tobermorite structure is naturally saturated with

Ca(II) [79], the immobilisation of U(VI) can take place on a short timescale and is very effective. In the long term, precipitation or incorporation in the C-S-H phase's structure of U(VI) as described by Harfouche et al. [52] and Tits et al. [57] may also take place, leading to an almost irreversible retention behaviour.

Table 3. Distribution coefficients R_d for the retention of $5 \cdot 10^{-7}$ mol·L^{-1} U(VI) on Circosil$^®$ in 0.1 M NaCl (pH 10.9) and diluted Gipshut solution (DGS, pH 10.6) at ten different sampling times (also in the presence of $5 \cdot 10^{-7}$ mol·L^{-1} Sm(III), Eu(III), Cs(I), Zr(IV), Ru(III), Mo(VI) and Pd(II)).

Equilibration Time [d]	R_d(U(VI)) in 0.1 M NaCl [10^3 L·kg^{-1}]	R_d(U(VI)) in DGS [10^3 L·kg^{-1}]
0.04	0.34 ± 0.06	0.24 ± 0.09
1	1.8 ± 0.7	1.9 ± 1.4
3	5 ± 2.4	1.2 ± 0.1
7	19 ± 10	4.2 ± 1.1
14	71 ± 17	5.3 ± 3.2
28	71 ± 20	12 ± 12
56	19 ± 20	7 ± 4
112	2.8 ± 0.5	3.2 ± 0.7
168	110 ± 76	>100 *
217	210 ± 200	4 ± 2

*At least one of the triplicates was below the detection limit.

In 0.1 M NaCl, $2.8 \pm 1.2 \cdot 10^{-3}$ mol·L^{-1} Ca(II) is leached out of Circosil$^®$ after 7 d in the presence of the WC. In DGS, the leaching is with $4.6 \pm 1.0 \cdot 10^{-3}$ mol·L^{-1} Ca(II) more effective due to the amount of competing ions, e.g., Na(I), displacing Ca(II) from the C-S-H phase's surface. Older results on the influence of ionic strength on Ca(II) leaching from Portland cement show a similar trend, where in 0.1 M NaCl solution $3.0 \pm 0.1 \cdot 10^{-3}$ mol·L^{-1} Ca(II) and in 2.5 M NaCl $3.8 \pm 0.1 \cdot 10^{-3}$ mol·L^{-1} Ca(II) are leached out of the cement after 72 h [80]. Therefore, here, in DGS, less Ca(II) is accessible to form Ca-O-U-bridges and the retention of U(VI) decreases slightly. Nevertheless, there is still enough Ca(II) on the Circosil$^®$ surface left to immobilise the major part (>94%) of U(VI).

A comparison between the present study and a kinetic study on a wet chemical synthesised C-S-H phase (C/S = 1.08) shows similarities of the retention behaviour of U(VI) in DGS [14]. In that study, U(VI) retention increases fast and reaches a first steady state after 7 d. This contradicts literature where a higher C/S ratio leads to a lower U(VI) immobilisation [51] but is in good agreement with Tits et al. [9]. The retention of U(VI) is slightly slower at the higher C/S ratio in 0.1 M NaCl than in the current study [14]. This, again, agrees with the findings of Pointeau et al. [51]. It seems that decreasing U(VI) immobilisation with increasing C/S ratio is valid for low ionic strength but reverses at higher salinity. Ochs et al. [3] explained the decrease in U(VI) retention with increasing C/S ratio with Ca(II) occupying binding sites for U(VI) but the results in DGS and in the literature [30,55,56] show that the presence of Ca(II) enhances the immobilisation of U(VI). The decrease may be caused by the increasing OH$^-$ concentration somehow interfering with the U(VI) retention on the C-S-H phase's surface. Another explanation could be the formation of a Ca(II)-U(VI) species in solution before the immobilisation takes place. This takes the decreasing immobilisation of U(VI) with increasing C/S ratio into account as well as the increasing immobilisation in the presence of Ca(II) in solution.

It is remarkable that three different kinetic studies on U(VI) and Eu(III) show different adsorption kinetics comparing both elements. Burešová et al. [44] noticed a faster immobilisation of Eu(III) than U(VI). Baur et al. [14] observed retention on the same timescale and, in the present study, U(VI) becomes immobilised faster than Eu(III). The main difference is the time Eu(III) needs to reach a steady state. With more competing ions present in solution, Eu(III) needs more time for immobilisation. This is firstly a direct hint of a retention mechanism for Eu(III) where competing ions play a role, e.g., adsorption or

incorporation. Secondly, it indicates the necessity of investigating element mixtures instead of solely single-element studies.

4. Conclusions

This study shows that the retention of the investigated elements on the commercial and hydrothermal synthesised C-S-H phase Circosil®, which is stable against CO_2, is comparable with the retention on wet chemical synthesised C-S-H phases. This is shown by the obtained R_d values. To the best of our knowledge, this is the first time the retention behaviour of eight repository relevant elements combined as a WC was studied, especially under alkaline and high-saline conditions. Additionally, this time-dependent study delivers new findings on the retention mechanisms in the nanomolar concentration range.

For Cs(I), discrepancies between commercial and wet chemical synthesised C-S-H phases can be seen, e.g., compared to the similar study of Baur et al. [14]. But there are many contradicting studies concerning the adsorption of Cs(I) on C-S-H phases in the literature. Many factors can possibly influence the Cs(I) retention: C/S ratio, amorphousness, reversibility of the adsorption process, solid-to-liquid ratio, salinity and competing ions. Under the used conditions, moderate and irreversible uptake of Cs(I) on Circosil® could be shown in 0.1 M NaCl (75 ± 1%). The adsorption is with 14 ± 1% lower in DGS and decreases slowly after 112 d. Unfortunately, a direct impact of the WC elements was not visible due to the highly saline background electrolytes. A direct comparison between single-element and WC experiments or additional studies in lower-saline solutions or with higher concentrations of the competing ions are necessary to elucidate the pure influence of the radioactive inventory in HLW disposal.

The present study proves that precipitation (e.g., as $Na_2U_2O_7$ or $CaUO_4$) can be excluded as initial retention mechanism for U(VI) on Circosil® in the nanomolar concentration range. Competing ions from the WC itself or from the background electrolytes only slightly influence the strong and irreversible retention. Compared to the literature, the role of the C/S ratio, Ca(II) concentration and pH value in the immobilisation kinetics needs further investigation.

The preferred retention of Sm(III) and Eu(III) on Circosil® over precipitation and wall adsorption could clearly be seen. The wall adsorption decreased from >90% in 0.1 M NaCl and >60% in DGS to <15% in the presence of the C-S-H phase. Combined with the findings of the kinetic study where increasing salinity leads to decreasing retention of Sm(III) and Eu(III), it can be concluded that surface complexation is the initial immobilisation mechanism for both elements. Furthermore, the slower kinetics compared to previous studies suggests a competing effect, e.g., between Eu(III), Sm(III) and Ru(III). A concentration series can be useful for further clarification.

Author Contributions: Conceptualisation, K.B. and R.K.; methodology, K.B.; validation, K.B., A.H. and R.K.; formal analysis, K.B.; investigation, K.B. and A.H.; writing—original draft preparation, K.B.; writing—review and editing, K.B., A.H. and R.K.; visualisation, K.B.; supervision, R.K.; project administration, R.K.; funding acquisition, R.K. All authors have read and agreed to the published version of the manuscript.

Data Availability Statement: Data available on request from the authors.

Conflicts of Interest: The authors declare no conflict of interest.

References

1. Atkins, M.; Glasser, F.P.; Kindness, A. Cement hydrate phase: Solubility at 25 °C. *Cem. Concr. Res.* **1992**, *22*, 241–246. [CrossRef]
2. Evans, N.D.M. Binding mechanisms of radionuclides to cement. *Cem. Concr. Res.* **2008**, *38*, 543–553. [CrossRef]

3. Ochs, M.; Mallants, D.; Wang, L. *Radionuclide and Metal Sorption on Cement and Concrete*, 1st ed.; Springer: Cham, Switzerland, 2016.

4. Jacques, D. *Time Dependence of the Geochemical Boundary Conditions for the Cementitious Engineered Barriers of the Belgian Surface Disposal Facility*; NIROND-TR 2008-24E; ONDRAF: Brussels, Belgium, 2008.

5. Lothenbach, B.; Nonat, A. Calcium silicate hydrates: Solid and liquid phase composition. *Cem. Concr. Res.* **2015**, *78*, 57–70. [CrossRef]

6. Gaona, X.; Dähn, R.; Tits, J.; Scheinost, A.C.; Wieland, E. Uptake of Np(IV) by C–S–H Phases and Cement Paste: An EXAFS Study. *Environ. Sci. Technol.* **2011**, *45*, 8765–8771. [CrossRef]

7. Tits, J.; Wieland, E.; Müller, C.J.; Landesman, C.; Bradbury, M.H. Strontium binding by calcium silicate hydrates. *J. Colloid Interface Sci.* **2006**, *300*, 78–87. [CrossRef]

8. Chen, J.J.; Thomas, J.J.; Taylor, H.F.W.; Jennings, H.M. Solubility and structure of calcium silicate hydrate. *Cem. Concr. Res.* **2004**, *34*, 1499–1519. [CrossRef]

9. Tits, J.; Fujita, T.; Tsukamoto, M.; Wieland, E. Uranium(VI) Uptake by Synthetic Calcium Silicate Hydrates. *Mater. Res. Soc. Symp. Proc.* **2008**, *1107*, 467. [CrossRef]

10. Kaja, A.M.; Delsing, A.; van der Laan, S.R.; Brouwers, H.J.H.; Yu, Q. Effects of carbonation on the retention of heavy metals in chemically activated BOF slag pastes. *Cem. Concr. Res.* **2021**, *148*, 106534. [CrossRef]

11. Ke, X.; Bernal, S.A.; Provis, J.L.; Lothenbach, B. Thermodynamic modelling of phase evolution in alkali-activated slag cements exposed to carbon dioxide. *Cem. Concr. Res.* **2020**, *136*, 106158. [CrossRef]

12. Steiner, S.; Lothenbach, B.; Proske, T.; Borgschulte, A.; Winnefeld, F. Effect of relative humidity on the carbonation rate of portlandite, calcium silicate hydrates and ettringite. *Cem. Concr. Res.* **2020**, *135*, 106116. [CrossRef]

13. Cirkel GmbH & Co. KG. *Product Information: Circosil®*; Cirkel GmbH & Co. KG: Emsdetten, Germany, 2019.

14. Baur, S.; Brix, K.; Feuerstein, A.; Janka, O.; Kautenburger, R. Retention of waste cocktail elements onto characterised calcium silicate hydrate (C–S–H) phases: A kinetic study under highly saline and hyperalkaline conditions. *Appl. Geochem.* **2022**, *143*, 105319. [CrossRef]

15. Schade, T. *Analyse und Modellierung der Einflussfaktoren Schnell Erstarrender Hochfester Anorganischer Verbundmörtel*; Kassel University Press: Kassel, Germany, 2021.

16. Richardson, I. Model structures for C-(A)-S-H(I). *Acta Crystallogr. B* **2014**, *70*, 903–923. [CrossRef] [PubMed]

17. Richardson, I.G. The calcium silicate hydrates. *Cem. Concr. Res.* **2008**, *38*, 137–158. [CrossRef]

18. Jackson, M.D.; Chae, S.R.; Mulcahy, S.R.; Meral, C.; Taylor, R.; Li, P.; Emwas, A.-H.; Moon, J.; Yoon, S.; Vola, G.; et al. Unlocking the secrets of Al-tobermorite in Roman seawater concrete. *Am. Miner.* **2013**, *98*, 1669–1687. [CrossRef]

19. Jackson, M.D.; Mulcahy, S.R.; Chen, H.; Li, Y.; Li, Q.; Cappelletti, P.; Wenk, H.-R. Phillipsite and Al-tobermorite mineral cements produced through low-temperature water-rock reactions in Roman marine concrete. *Am. Miner.* **2017**, *102*, 1435–1450. [CrossRef]

20. Collins, E.D.; DelCul, G.D.; Spencer, B.B.; Brunson, R.R.; Johnson, J.A.; Terekhov, D.S.; Emmanuel, N.V. Process Development Studies for Zirconium Recovery/Recycle from used Nuclear Fuel Cladding. *Procedia Chem.* **2012**, *7*, 72–76. [CrossRef]

21. Motta, A.T.; Couet, A.; Comstock, R.J. Corrosion of Zirconium Alloys Used for Nuclear Fuel Cladding. *Annu. Revi. Mater. Res.* **2015**, *45*, 311–343. [CrossRef]

22. Anderson, W.K. Broad Aspects of Absorber Materials Selection for Reactor Control. *Nucl. Sci. Eng.* **1958**, *4*, 357–372. [CrossRef]

23. Johnston, H.F.; Russell, J.L.; Silvernail, W.L. Relative Control Rod Worths of Some Rare Earth Oxides. *Nucl. Sci. Eng.* **1959**, *6*, 93–96. [CrossRef]

24. Eisenbud, M.; Krauskopf, K.; Franca, E.P.; Lei, W.; Ballad, R.; Linsalata, P.; Fujimori, K. Natural analogues for the transuranic actinide elements: An investigation in Minas Gerais, Brazil. *Environ. Geol. Water Sci.* **1984**, *6*, 1–9. [CrossRef]

25. Krauskopf, K.B. Thorium and rare-earth metals as analogs for actinide elements. *Chem. Geol.* **1986**, *55*, 323–335. [CrossRef]

26. Tits, J.; Stumpf, T.; Rabung, T.; Wieland, E.; Fanghänel, T. Uptake of Cm(III) and Eu(III) by Calcium Silicate Hydrates: A Solution Chemistry and Time-Resolved Laser Fluorescence Spectroscopy Study. *Environ. Sci. Technol.* **2003**, *37*, 3568–3573. [CrossRef] [PubMed]

27. Hama, K.; Kunimaru, T.; Metcalfe, R.; Martin, A.J. The hydrogeochemistry of argillaceous rock formations at the Horonobe URL site, Japan. *Phys. Chem. Earth Parts A/B/C* **2007**, *32*, 170–180. [CrossRef]

28. Nguyen, X.P.; Cui, Y.J.; Tang, A.M.; Deng, Y.F.; Li, X.L.; Wouters, L. Effects of pore water chemical composition on the hydro-mechanical behavior of natural stiff clays. *Eng. Geol.* **2013**, *166*, 52–64. [CrossRef]

29. Van Loon, L.R.; Baeyens, B.; Bradbury, M.H. Diffusion and retention of sodium and strontium in Opalinus clay: Comparison of sorption data from diffusion and batch sorption measurements, and geochemical calculations. *Appl. Geochem.* **2005**, *20*, 2351–2363. [CrossRef]

30. Brix, K.; Baur, S.; Haben, A.; Kautenburger, R. Building the bridge between U(VI) and Ca-bentonite—Influence of concentration, ionic strength, pH, clay composition and competing ions. *Chemosphere* **2021**, *285*, 131445. [CrossRef]

31. Brix, K.; Hein, C.; Haben, A.; Kautenburger, R. Adsorption of caesium on raw Ca-bentonite in high saline solutions: Influence of concentration, mineral composition, other radionuclides and modelling. *Appl. Clay Sci.* **2019**, *182*, 105275. [CrossRef]

32. Kautenburger, R.; Brix, K.; Hein, C. Insights into the retention behaviour of europium(III) and uranium(VI) onto Opalinus Clay influenced by pore water composition, temperature, pH and organic compounds. *Appl. Geochem.* **2019**, *109*, 104404. [CrossRef]

33. Liu, C.; Zachara, J.M.; Smith, S.C. A cation exchange model to describe Cs+ sorption at high ionic strength in subsurface sediments at Hanford site, USA. *J. Contam. Hydrol.* **2004**, *68*, 217–238. [CrossRef]

34. Yan, Y.; Bernard, E.; Miron, G.D.; Rentsch, D.; Ma, B.; Scrivener, K.; Lothenbach, B. Kinetics of Al uptake in synthetic calcium silicate hydrate (C-S-H). *Cem. Concr. Res.* **2023**, *172*, 107250. [CrossRef]

35. Yan, Y.; Ma, B.; Miron, G.D.; Kulik, D.A.; Scrivener, K.; Lothenbach, B. Al uptake in calcium silicate hydrate and the effect of alkali hydroxide. *Cem. Concr. Res.* **2022**, *162*, 106957. [CrossRef]

36. Iwaida, T.; Nagasaki, S.; Tanaka, S.; Yaita, T.; Tachimori, S. Structure alteration of C-S-H (calcium silicate hydrated phases) caused by sorption of caesium. *Radiochim. Acta* **2002**, *90*, 677–681. [CrossRef]

37. Missana, T.; García-Gutiérrez, M.; Mingarro, M.; Alonso, U. Comparison between cesium and sodium retention on calcium silicate hydrate (CSH) phases. *Appl. Geochem.* **2018**, *98*, 36–44. [CrossRef]

38. Atkinson, A.; Nickerson, A.K. Diffusion and Sorption of Cesium, Strontium, and Iodine in Water-Saturated Cement. *Nucl. Technol.* **1988**, *81*, 100–113. [CrossRef]

39. Duque-Redondo, E.; Kazuo, Y.; López-Arbeloa, I.; Manzano, H. Cs-137 immobilization in C-S-H gel nanopores. *Phys. Chem. Chem. Phys.* **2018**, *20*, 9289–9297. [CrossRef]

40. Heath, T.G.; Ilett, D.J.; Tweed, C.J. Thermodynamic Modelling of the Sorption of Radioelements onto Cementitious Materials. *Mater. Res. Soc. Symp. Proc. OPL* **1995**, *412*, 443. [CrossRef]

41. Jiang, J.; Wang, P.; Hou, D. The mechanism of cesium ions immobilization in the nanometer channel of calcium silicate hydrate: A molecular dynamics study. *Phys. Chem. Chem. Phys.* **2017**, *19*, 27974–27986. [CrossRef]

42. Missana, T.; García-Gutiérrez, M.; Mingarro, M.; Alonso, U. Analysis of barium retention mechanisms on calcium silicate hydrate phases. *Cem. Concr. Res.* **2017**, *93*, 8–16. [CrossRef]

43. Viallis, H.; Faucon, P.; Petit, J.C.; Nonat, A. Interaction between Salts (NaCl, CsCl) and Calcium Silicate Hydrates (C–S–H). *J. Phys. Chem. B* **1999**, *103*, 5212–5219. [CrossRef]

44. Burešová, M.; Kittnerová, J.; Drtinová, B. Comparative study of Eu and U sorption on cementitious materials in the presence of organic substances. *J. Radioanal. Nucl. Chem.* **2023**, *332*, 1499–1504. [CrossRef]

45. Dettmann, S.; Huittinen, N.M.; Jahn, N.; Kretzschmar, J.; Kumke, M.U.; Kutyma, T.; Lohmann, J.; Reich, T.; Schmeide, K.; Shams Aldin Azzam, S.; et al. Influence of gluconate on the retention of Eu(III), Am(III), Th(IV), Pu(IV), and U(VI) by C-S-H (C/S = 0.8). *Front. Nucl. Eng.* **2023**, *2*, 1124856. [CrossRef]

46. Mandaliev, P.; Stumpf, T.; Tits, J.; Dähn, R.; Walther, C.; Wieland, E. Uptake of Eu(III) by 11Å tobermorite and xonotlite: A TRLFS and EXAFS study. *Geochim. Cosmochim. Acta* **2011**, *75*, 2017–2029. [CrossRef]

47. Pointeau, I.; Piriou, B.; Fedoroff, M.; Barthes, M.G.; Marmier, N.; Fromage, F. Sorption Mechanisms of Eu(3+) on CSH Phases of Hydrated Cements. *J. Colloid Interface Sci.* **2001**, *236*, 252–259. [CrossRef] [PubMed]

48. Schlegel, M.L.; Pointeau, I.; Coreau, N.; Reiller, P. Mechanism of Europium Retention by Calcium Silicate Hydrates: An EXAFS Study. *Environ. Sci. Technol.* **2004**, *38*, 4423–4431. [CrossRef]

49. Macé, N.; Page, J.; Reiller, P.E. Uranium(VI) Sorption onto Hardened Cement Paste under High Saline and Alkaline Conditions. *Minerals* **2023**, *13*, 325. [CrossRef]

50. Philipp, T.; Shams Aldin Azzam, S.; Rossberg, A.; Huittinen, N.; Schmeide, K.; Stumpf, T. U(VI) sorption on Ca-bentonite at (hyper)alkaline conditions—Spectroscopic investigations of retention mechanisms. *Sci. Total Environ.* **2019**, *676*, 469–481. [CrossRef]

51. Pointeau, I.; Landesman, C.; Giffaut, E.; Reiller, P. Reproducibility of the uptake of U(VI) onto degraded cement pastes and calcium silicate hydrate phases. *Radiochim. Acta* **2004**, *92*, 645–650. [CrossRef]

52. Harfouche, M.; Wieland, E.; Dähn, R.; Fujita, T.; Tits, J.; Kunz, D.; Tsukamoto, M. EXAFS study of U(VI) uptake by calcium silicate hydrates. *J. Colloid Interface Sci.* **2006**, *303*, 195–204. [CrossRef]

53. Androniuk, I.; Landesman, C.; Henocq, P.; Kalinichev, A.G. Adsorption of gluconate and uranyl on C-S-H phases: Combination of wet chemistry experiments and molecular dynamics simulations for the binary systems. *Phys. Chem. Earth Parts A/B/C* **2017**, *99*, 194–203. [CrossRef]

54. Baqer, Y.; Thornton, S.; Stewart, D.I.; Norris, S.; Chen, X. Analysis of Uranium Sorption in a Laboratory Column Experiment Using a Reactive Transport and Surface Complexation Model. *Transp. Porous Media* **2023**, *149*, 423–452. [CrossRef]

55. Androniuk, I.; Kalinichev, A.G. Molecular dynamics simulation of the interaction of uranium (VI) with the C–S–H phase of cement in the presence of gluconate. *Appl. Geochem.* **2020**, *113*, 104496. [CrossRef]

56. Philipp, T.; Huittinen, N.; Shams Aldin Azzam, S.; Stohr, R.; Stietz, J.; Reich, T.; Schmeide, K. Effect of Ca(II) on U(VI) and Np(VI) retention on Ca-bentonite and clay minerals at hyperalkaline conditions—New insights from batch sorption experiments and luminescence spectroscopy. *Sci. Total Environ.* **2022**, *842*, 156837. [CrossRef] [PubMed]

57. Tits, J.; Walther, C.; Stumpf, T.; Macé, N.; Wieland, E. A luminescence line-narrowing spectroscopic study of the uranium(vi) interaction with cementitious materials and titanium dioxide. *Dalton Trans.* **2015**, *44*, 966–976. [CrossRef]

58. Altmaier, M.; Metz, V.; Neck, V.; Müller, R.; Fanghänel, T. Solid-liquid equilibria of Mg(OH)2(cr) and Mg2(OH)3Cl·4H2O(cr) in the system Mg-Na-H-OH-Cl-H2O at 25 °C. *Geochim. Cosmochim. Acta* **2003**, *67*, 3595–3601. [CrossRef]

59. Hein, C.; Sander, J.M.; Kautenburger, R. New approach of a transient ICP-MS measurement method for samples with high salinity. *Talanta* **2017**, *164*, 477–482. [CrossRef]

60. Ball, J.W.; Nordstrom, D.K. *User's Manual for WATEQ4F, with Revised Thermodynamic Data Base and Text Cases for Calculating Speciation of Major, Trace, and Redox Elements in Natural Waters*; US Geological Survey: Reston, VA, USA, 1991; pp. 91–183.

61. Diakonov, I.I.; Ragnarsdottir, K.V.; Tagirov, B.R. Standard thermodynamic properties and heat capacity equations of rare earth hydroxides:: II. Ce(III)-, Pr-, Sm-, Eu(III)-, Gd-, Tb-, Dy-, Ho-, Er-, Tm-, Yb-, and Y-hydroxides. Comparison of thermochemical and solubility data. *Chem. Geol.* **1998**, *151*, 327–347. [CrossRef]

62. Spahiu, K.; Bruno, J. *A Selected Thermodynamic Database for REE to be Used in HLNW Performance Assessment Exercises*; 0284-3757; Fuel and Waste Management Co.: Stockholm, Sweden, 1995; p. 90.

63. Altmaier, M.; Yalçıntaş, E.; Gaona, X.; Neck, V.; Müller, R.; Schlieker, M.; Fanghänel, T. Solubility of U(VI) in chloride solutions. I. The stable oxides/hydroxides in NaCl systems, solubility products, hydrolysis constants and SIT coefficients. *J. Chem. Thermodyn.* **2017**, *114*, 2–13. [CrossRef]

64. Plancque, G.; Moulin, V.; Toulhoat, P.; Moulin, C. Europium speciation by time-resolved laser-induced fluorescence. *Anal. Chim. Acta* **2003**, *478*, 11–22. [CrossRef]

65. Pointeau, I.; Marmier, N.; Fromage, F.; Fedoroff, M.; Giffaut, E. Cesium and Lead Uptake by CSH Phases of Hydrated Cement. *Mater. Res. Soc. Symp. Proc.* **2000**, *663*, 97. [CrossRef]

66. Arayro, J.; Dufresne, A.; Zhou, T.; Ioannidou, K.; Ulm, J.-F.; Pellenq, R.; Béland, L.K. Thermodynamics, kinetics, and mechanics of cesium sorption in cement paste: A multiscale assessment. *Phys. Rev. Mater.* **2018**, *2*, 053608. [CrossRef]

67. Duque-Redondo, E.; Yamada, K.; Manzano, H. Cs retention and diffusion in C-S-H at different Ca/Si ratio. *Cem. Concr. Res.* **2021**, *140*, 106294. [CrossRef]

68. Park, S.M.; Jang, J.G. Carbonation-induced weathering effect on cesium retention of cement paste. *J. Nucl. Mater.* **2018**, *505*, 159–164. [CrossRef]

69. Komarneri, S.; Roy, D.M.; Roy, R. Al-substituted tobermorite: Shows cation exchange. *Cem. Concr. Res.* **1982**, *12*, 773–780. [CrossRef]

70. Tsutsumi, T.; Nishimoto, S.; Kameshima, Y.; Miyake, M. Hydrothermal preparation of tobermorite from blast furnace slag for Cs+ and Sr2+ sorption. *J. Hazard. Mater.* **2014**, *266*, 174–181. [CrossRef] [PubMed]

71. Bach, T.T.H.; Chabas, E.; Pochard, I.; Cau Dit Coumes, C.; Haas, J.; Frizon, F.; Nonat, A. Retention of alkali ions by hydrated low-pH cements: Mechanism and Na$^+$/K$^+$ selectivity. *Cem. Concr. Res.* **2013**, *51*, 14–21. [CrossRef]

72. Cornell, R.M. Adsorption of cesium on minerals: A review. *J. Radioanal. Nucl. Chem.* **1993**, *171*, 483–500. [CrossRef]

73. Vejsada, J.; Hradil, D.; Řanda, Z.; Jelínek, E.; Štulík, K. Adsorption of cesium on Czech smectite-rich clays—A comparative study. *Appl. Clay Sci.* **2005**, *30*, 53–66. [CrossRef]

74. Bu, J.; Gonzalez Teresa, R.; Brown, K.G.; Sanchez, F. Adsorption mechanisms of cesium at calcium-silicate-hydrate surfaces using molecular dynamics simulations. *J. Nucl. Mater.* **2019**, *515*, 35–51. [CrossRef]

75. Li, K.; Pang, X. Sorption of radionuclides by cement-based barrier materials. *Cem. Concr. Res.* **2014**, *65*, 52–57. [CrossRef]

76. Ali, O.I.M.; Osman, H.H.; Sayed, S.A.; Shalabi, M.E.H. The removal of some rare earth elements from their aqueous solutions on by-pass cement dust (BCD). *J. Hazard. Mater.* **2011**, *195*, 62–67. [CrossRef]

77. Häußler, V.; Amayri, S.; Beck, A.; Platte, T.; Stern, T.A.; Vitova, T.; Reich, T. Uptake of actinides by calcium silicate hydrate (C-S-H) phases. *Appl. Geochem.* **2018**, *98*, 426–434. [CrossRef]

78. Pointeau, I.; Coreau, N.; Reiller, P.E. Uptake of anionic radionuclides onto degraded cement pastes and competing effect of organic ligands. *Radiochim. Acta* **2008**, *96*, 367–374. [CrossRef]

79. Zhang, N.; Carrez, P.; Shahsavari, R. Screw-Dislocation-Induced Strengthening–Toughening Mechanisms in Complex Layered Materials: The Case Study of Tobermorite. *ACS Appl. Mater. Interfaces* **2017**, *9*, 1496–1506. [CrossRef]

80. Boulard, L.; Kautenburger, R. Short-term elemental release from Portland cement concrete in hypersaline leaching conditions. *Adv. Cem. Res.* **2020**, *32*, 148–157. [CrossRef]